Strongly Coupled Magnons and Cavity Microwave Photons

Xufeng Zhang,[1] Chang-Ling Zou,[2,3] Liang Jiang,[2] and Hong X. Tang[1,*]
[1]Department of Electrical Engineering, Yale University, New Haven, Connecticut 06511, USA
[2]Department of Applied Physics, Yale University, New Haven, Connecticut 06511, USA
[3]Key Lab of Quantum Information, University of Science and Technology of China, Hefei 230026, Anhui, People's Republic of China
(Received 27 May 2014; published 7 October 2014)

We realize a cavity magnon-microwave photon system in which a magnetic dipole interaction mediates strong coupling between the collective motion of a large number of spins in a ferrimagnet and the microwave field in a three-dimensional cavity. By scaling down the cavity size and increasing the number of spins, an ultrastrong coupling regime is achieved with a cooperativity reaching 12 600. Interesting dynamic features including classical Rabi-like oscillation, magnetically induced transparency, and the Purcell effect are demonstrated in this highly versatile platform, highlighting its great potential for coherent information processing.

DOI: 10.1103/PhysRevLett.113.156401 PACS numbers: 71.36.+c, 42.50.Pq, 75.30.Ds, 76.50.+g

Introduction.—Systems with strong light-matter interaction have played crucial roles in quantum [1,2] and classical information processing [3,4] as they enable coherent information transfer between distinct physical platforms. It is well known that systems with a large electric dipole moment can couple strongly with the optical fields. However, the possibility of strong light-matter interaction via magnetic dipoles is mostly ignored. It is only recently that Imamoglu [5] has pointed out the direction to achieve strong light-matter interaction using collective excitations of spin ensembles, and envisioned the promise of quantum information processing in these systems. Since then, various implementations have been proposed and experimentally investigated. Ensembles including ultracold atomic clouds [6], molecules [7], nitrogen vacancy centers in diamond [8–13], and ion doped crystals [14–16], have been used to couple to microwave resonators or even superconducting qubits.

Magnetic materials provide a promising alternative to achieve strong light-matter interaction, because they have spin density many orders of magnitude higher than the dilute spin ensembles investigated previously. For example, Soykal *et al.* [17,18] predicted that the nanomagnet-photon cavity can achieve strong light-matter interaction assisted by an extremely large number of spins in nanomagnets. In this Letter, we realize such a hybrid system, which consists of a sphere of yttrium iron garnet (YIG, $Y_3Fe_5O_{12}$) and a three-dimensional (3D) microwave cavity. This new system possesses several distinguishing advantages. First, YIG has a high spin density ($\rho_s = 4.22 \times 10^{27}$ m^{-3}) exceeding previous spin ensembles by several orders of magnitude. Second, spin excitations in single crystal and highly purified YIG possess a very low damping rate. Third, the spin-spin interactions through either exchange or dipolar interactions give rise to dispersions of spin excitations (defined modes) in YIG, which can be used for spatial multiplexing. It is also intriguing that there is nonlinear interaction between excitations in the YIG, which enables nonlinear amplification and the control of magnons. For instance, Bose-Einstein condensates of quasiequilibrium magnons have been realized at room temperature [19].

With the proposed hybrid system, we experimentally demonstrate the coherent coupling between magnons (the collective spin excitation in YIG) and microwave photons. Because of the large spin number in YIG, strong coupling can be achieved. An experimental demonstration has been previously reported using a YIG thin film on a planar superconducting microwave cavity, and a high cooperativity of 1350 has been achieved [20]. Here, we show that by utilizing a spherical YIG geometry and 3D microwave cavity, our system obtains additional advantages such as more uniform coupling and higher quality (Q) factors [21–23], which allow the strong coupling to take place even at room temperature. Furthermore, our 3D system is highly tunable in various parameters, which allows us to observe characteristic phenomena associated with distinct parameter regimes, including the magnetically induced transparency (MIT, the magnetic analog of EIT, the electromagnetically induced transparency) and the Purcell effect. Moreover, by scaling the device dimensions, our 3D system can enter the so-called "ultrastrong coupling" (USC) regime, where the coupling rate reaches a large fraction of the oscillation frequency [24–31]. Although these important features are measured in the classical regime at room temperature, our results suggest important prospects of operating the coupled system in the quantum regime at millikelvins where the ferromagnetic resonance linewidth of YIG can go down to 1.5 μT [32] with the magnon lifetime extended to as long as about 4 μs.

Experimental setup.—The image of our device is shown in the bottom of Fig. 1(a), consisting of a 3D microwave cavity (only the bottom half is shown) and a highly

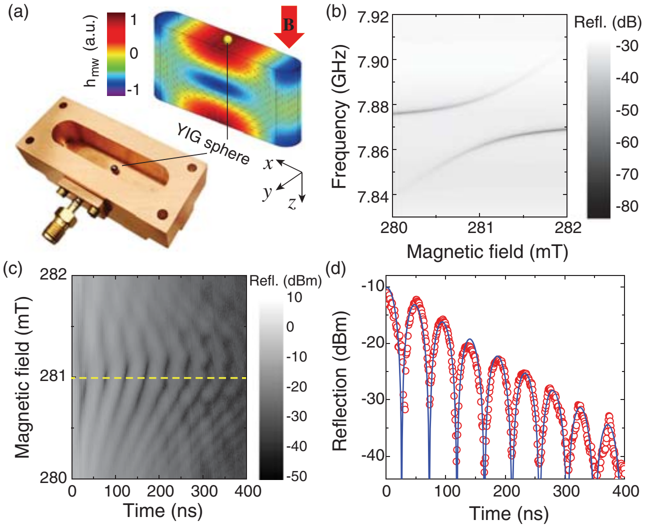

FIG. 1 (color online). (a) Top: Simulated microwave cavity resonance TE101 mode distribution. The red arrows and colors indicate the magnetic field directions and amplitudes, respectively. Bottom: Device image showing half of the microwave cavity with a YIG sphere inside. (b) Measured normal mode splitting spectrum as a function of the bias magnetic field. (c) The evolution of the cavity energy after a pulse excitation at the varying bias magnetic field. (d) The measured Rabi-like oscillation signal at the zero detuned bias magnetic field. Red circles: Measurement results. Solid blue line: Theoretical calculation using parameters obtained from the normal mode splitting spectrum.

polished YIG sphere which serves as the magnon cavity. The microwave cavity is a box machined from high conductivity copper to obtain a high Q factor at room temperature. For example, the box with an inner dimension of $43.0 \times 21.0 \times 9.6\ \mathrm{mm}^3$ gives a TE101 mode at $\omega/2\pi = 7.875$ GHz with a linewidth of a few MHz. The simulated mode distribution (using COMSOL 3.5) of the cavity mode is given in the top of Fig. 1(a), where the arrows and colors indicate the magnetic field directions and their amplitudes. The spectroscopic measurement is carried out with a vector network analyzer by probing the reflection of the microwave cavity through a coaxial cable antenna.

The YIG sphere is placed inside the microwave cavity and biased with a static magnetic field, $\vec{B}_0$. The magnetic components of the microwave field perpendicular to the bias field induce the spin flip, and thus excite the magnon mode in YIG. Here, we are only interested in the lowest order ferromagnetic resonance mode, which is a uniform collective mode that all the spins precess in phase. This mode has the highest coupling strength given that the microwave magnetic field around the YIG sphere is approximately uniform [Fig. 1(a)] as the wavelength $\lambda_{mw} \gg R$ with R is the radius of the YIG sphere. The frequency of the uniform magnon mode linearly depends on the bias field: $\omega_m = \gamma|\vec{B}_0| + \omega_{m,0}$, where $\gamma = 28$ GHz/T is the gyromagnetic ratio and $\omega_{m,0}$ is determined by the anisotropy field. The bias magnetic field is tunable in the range of 0–2 T, corresponding to a magnon frequency from a few hundred MHz to about 50 GHz.

Strong coupling.—To study the microwave photon-magnon interaction, we adjust the bias field so that the magnon is near resonance with the cavity's TE101 mode. The strongest coupling strength is obtained by placing the YIG sphere (0.36 mm in diameter) at the position with the maximum microwave magnetic field. The measured microwave reflection spectra with respect to the bias magnetic field B_0 are plotted in Fig. 1(b), which exhibits an avoided crossing at $B_0 = 281$ mT. The interaction between the microwave photon and magnon can be described by the Hamiltonian with a rotating-wave approximation (RWA):

$$\mathcal{H}/\hbar = \omega_a a^\dagger a + \omega_m m^\dagger m + g(a^\dagger m + a m^\dagger), \qquad (1)$$

where $a^\dagger$ (a) is the creation (annihilation) operator for the microwave photon at frequency ω_a. For the magnon, the collective spin excitations are approximately represented by the boson operator $m^\dagger(m)$ with the Holstein-Primakoff approximation [33]. The coupling strength g between the two systems is

$$g = \frac{\eta}{2}\gamma\sqrt{\frac{\hbar\omega\mu_0}{V_a}}\sqrt{2Ns}, \qquad (2)$$

where ω is the resonance frequency and V_a is the mode volume of the microwave cavity resonance, μ_0 is the vacuum permeability, N is the total number of spins, and $s = (5/2)$ is the spin number of the ground state Fe^{3+} ion in YIG. The coefficient $\eta \leq 1$ describes the spatial overlap and polarization matching conditions between the microwave field and the magnon mode [34].

As shown in Fig. 1(b), the avoided crossing indicates the strong coupling between the microwave photon and the magnon, with the coupling strength: $g/2\pi = 10.8$ MHz. We can also extract the dissipation rates (HWHM) of both the microwave photon ($\kappa_a/2\pi = 1.35$ MHz) and the magnon ($\kappa_m/2\pi = 1.06$ MHz). The measured spectrum agrees well with the theoretical prediction of the reflection from the microwave cavity [34]:

$$r(\omega) = -1 + \frac{2\kappa_{a,1}}{i(\omega_a - \omega) + \kappa_a + \frac{g^2}{i(\omega_m - \omega) + \kappa_m}}, \qquad (3)$$

where $\kappa_{a,1}$ is the external coupling to the cavity. For the coupled oscillator model described by the Hamiltonian in Eq. (1), hybridized photon-magnon quasiparticles $A_\pm = \sqrt{1/2}(a \pm m)$ appear for $\omega_a = \omega_m$, with energies being $\omega_m \pm g$. When the coupling strength exceeds the dissipation rates ($g > \kappa_{a,m}$), the system reaches the classical strong coupling regime. With the experiment parameters, we obtain a cooperativity of $C = g^2/\kappa_a\kappa_m = 81$.

The strong coupling implies coherent dynamics between the photon and the magnon, such as Rabi-like oscillations. Hence, we investigated the temporal dynamics of photons in the strongly coupled system. Experimentally, by monitoring the time evolution of the cavity output after a short pulse excitation, we obtain the time traces that agree well with the theoretical prediction of Rabi-like oscillations [Fig. 1(c)]. The slight asymmetry about the bias magnetic field is due to the nonzero duration of the excitation pulse. Clearly, the cavity energy experiences periodic oscillation aside from the exponential decay, demonstrating the coherent energy exchange between photon and magnon. At $B_0 = 281$ mT, where the magnon is on resonance with the microwave photon, we have the highest signal extinction, indicating a complete energy exchange between the two systems. Also at this bias magnetic field, the oscillation period is the longest, corresponding to the narrowest gap (g/π) in the avoided crossing regime of the reflection spectrum. The time trace for $B_0 = 281$ mT is plotted in Fig. 1(d), showing an extinction ratio of more than 20 dB, and a period of 46 ns which agrees well with the coupling strength $\pi/g = 46.3$ ns. The calculated oscillation signal (solid line, see Ref. [34] for calculation details) using the coupling strength and the decay rate obtained from the frequency spectrum shows excellent agreement with the measured time trace (circles).

MIT and Purcell effects.—Besides strong coupling, the tunability of our proposed system enables us to access other characteristic effects of the coherent photon-magnon interaction. Depending on the relative value of the coupling strength and the dissipation rates, there are different coupling regimes [Fig. 2(b)]. We will focus on coherent interactions with $C = (g/\kappa_a)(g/\kappa_m) > 1$.

When the dissipation of the microwave cavity becomes dominant in the coupled system [Fig. 2(a), $\kappa_m < g < \kappa_a$], the avoided crossing feature in the measured spectrum will disappear. In the experiment, we use a 0.25-mm diameter YIG sphere and fill the copper cavity ($43.0\times 21.0 \times 7.1$ mm^3) with a microwave absorber (Eccosorb LS-30/SS3) to reach the bad-cavity limit. Note that the presence of the microwave absorber reduces the cavity frequency. In this case, as we tune the bias magnetic field, an MIT window passes through the broad microwave cavity resonance [Fig. 2(c)]. Depending on the detuning of the magnon frequency, the transparency window shows up as an asymmetric Fano shape or symmetric peak. When the impedance matching [$\kappa_{a,1} = \kappa_a/2$ in Eq. (3)] and on-resonance conditions are satisfied, the MIT window height is $|r(\omega_a)|^2 = (C/(1+C))^2$ and the linewidth is $\Delta = 2(1+C)\kappa_m$. When the magnon is tuned on resonance with the microwave photon [at $B_0 = 197.4$ mT, indicated by the dashed line in Fig. 2(c)], we have the maximum extinction with a Lorentzian-shaped transparency window that replicates the magnon resonance [Fig. 2(d)]. The measured transparency window has a peak height of half

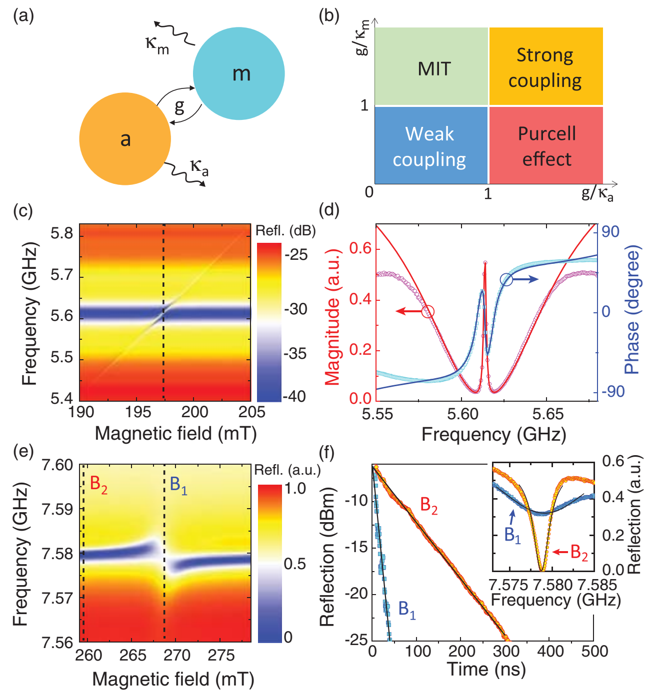

FIG. 2 (color online). (a) Schematic of the linearly coupled magnon (m) and photon (a) system. g, κ_m, κ_a are the coupling strength and dissipation rates of magnon and microwave cavity modes, respectively. (b) Different coupling regimes separated by the relative strength between the coupling rate and dissipation rates of the photon and magnon subsystems. (c) MIT spectrum at various bias magnetic fields. (d) Measured resonance spectrum (symbols) showing MIT at the zero detuning magnetic field. The solid lines are the theoretical fitting using Eq. (3). (e) Reflection spectrum showing the Purcell effect. (f) Cavity energy ringdown curves at two different bias magnetic fields B_1 (blue squares) and B_2 (red circles). Solid lines are the theoretical fittings. Inset: Resonance reflection spectra at B_1 (blue line) and B_2 (red line).

unity with a maximum group delay of 110 ns. From the measured data, the corresponding dissipation rates and the coupling strength are fitted using Eq. (3) as $\kappa_a/2\pi = 34.9$ MHz, $\kappa_m/2\pi = 0.24$ MHz, and $g/2\pi = 5.4$ MHz, corresponding to a cooperativity value of $C = 3.76$ for this specific device configuration.

On the other hand, when the magnon decay dominates [Fig. 2(a), $\kappa_a < g < \kappa_m$], we enter the Purcell regime with an enhanced decay of the microwave cavity photon due to its coupling to the lossy magnon. Lossy YIG spheres can be obtained by using rare-earth doped YIG, or alternatively, as in our experiments, gluing iron filings to the YIG sphere (1 mm in diameter) surface to introduce additional scattering and absorption loss. The cavity used here has a dimension of $40 \times 25 \times 15$ mm^3. According to Eq. (3), the effective dissipation rate of the cavity is $\kappa_a(1+C)$, enhanced by a Purcell factor ($F_P = C + 1$) as a result of the photon-magnon interaction. Such linewidth broadening is confirmed by the measured reflection spectra at various bias magnetic fields [Fig. 2(e)]. Although the magnon resonance cannot be resolved due to its large linewidth, its magnetic dependence is inherited by the coupled mode and shows up as a small bend. For a clear comparison, the resonance spectra of the microwave cavity with (at $B_1 = 268.4$ mT) and without (at $B_2 = 259.5$ mT) the coupling to the magnon are plotted in the inset of Fig. 2(f). Because of the Purcell effect, the dissipation rate of the microwave resonance ($\kappa_a/2\pi$) increases from 1.08 to 8.21 MHz. Thus, we have $F_P = 7.6$ and $C = 6.6$. From the experiment results, we can extract the coupling strength $g/2\pi \approx 15$ MHz and the magnon decay rate $\kappa_m/2\pi \approx 32$ MHz that indeed fall inside the Purcell regime.

A more direct characterization of such a Purcell effect is obtained by measuring the cavity photon lifetime. Since now the magnon dissipates very quickly, an accelerated exponential decay of the photon energy instead of a Rabi-like oscillation is expected after a pulsed excitation. The decay curves at bias magnetic fields B_1 and B_2 are plotted in Fig. 2(f), which gives a lifetime of $\tau_1 = 8.9 \pm 1.3$ ns and $\tau_2 = 72.2 \pm 0.3$ ns, respectively. These time domain measurements perfectly match the dissipation rates measured above in the frequency domain. Both the time and frequency domain measurements give a Purcell factor of about 8.

Ultrastrong coupling.—Beyond the four coupling regimes (discussed above) determined by the ratio of coupling strength and dissipation rates, there exists a USC regime where the coupling strength becomes considerably comparable with the magnon frequency. The USC has attracted intensive interest, being a potential playground for ultrafast coherent controlling and exploring new physics beyond RWA. It is notable that in our experiments, by engineering the microwave cavity and the YIG sphere, we can *tune* the coupling strength and eventually extend our coupled system to the USC regime. From Eq. (2) we can see that the coupling strength $g \propto \sqrt{\omega_{\mathrm{eff}}} = \sqrt{\omega_a (V_m/V_a)}$, where V_m is the volume of the YIG sphere which determines the spin number ($N \propto V_m$). By increasing the resonance frequency and the YIG sphere size while reducing the microwave cavity size, we can increase ω_{eff} and consequently the coupling strength g. The coupling strengths measured in ten devices of varying cavity and sphere dimensions are displayed in Fig. 3(a) as a function of ω_{eff}, where the black square corresponds to the data in Fig. 1 while the red star corresponds to the USC case. Good agreement is obtained in comparison with the theoretical prediction (solid line). During the experiments, different resonance frequencies ranging from the X band to the K_a band (7 to 40 GHz) are tested, showing the great tunability of the magnon.

An ultrastrong coupling strength of $g/2\pi = 2.5$ GHz has been achieved at a resonance frequency of $\omega_a/2\pi = 37.5$ GHz, where the microwave cavity size is dramatically reduced to $7.0\times5.0\times3.2\mathrm{mm}^3$, and the YIG sphere diameter is increased to 2.5 mm (corresponding to 3.5×10^{19} spins).

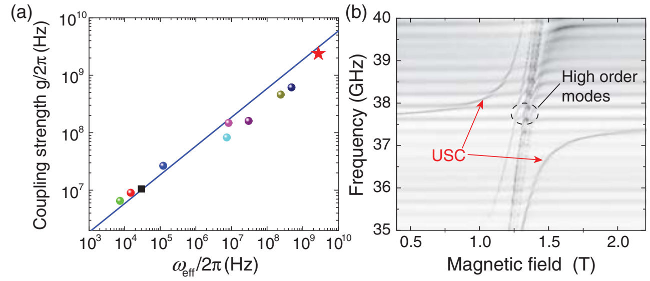

FIG. 3 (color online). (a) Coupling strength as a function of modal frequency, ω_{eff}. Solid line is the theoretical prediction. The red star indicates a device reaching the ultrastrong coupling. (b) Ultrastrong coupling spectrum in the K_a band. Red arrows show the ultrastrongly coupled magnon-microwave photon mode.

This coupled system yields a ratio of $g/\omega_a = 6.7\%$ and reaches the USC regime. Figure 3(b) plots the reflection spectrum of the USC. Because of the large YIG sphere size which is now comparable with the microwave cavity, the microwave fields penetrating the YIG sphere are no longer as uniform and therefore excite nonuniform magnon modes, as labeled in Fig. 3(b). These nonuniform modes have higher frequency, and mostly couple weakly with the microwave cavity. Also, at such high frequencies, the cavity resonance experiences higher losses. Nevertheless, due to the ultrahigh coupling rate, an ultrahigh cooperativity of $C \simeq 12600$ is realized with the extracted dissipation rates of the microwave photon and the magnon resonance are $\kappa_a/2\pi = 33$ MHz and $\kappa_m/2\pi = 15$ MHz, respectively.

Conclusion.—We have experimentally realized coherent coupling between microwave photon and magnon at room temperature, and demonstrated the great potential of magnon as an information carrier. Strong coupling with high cooperativity has been achieved using a spectroscopic measurement, and the coherent energy exchange has been illustrated with the Rabi-like oscillation measurement in the time domain. Both the MIT and Purcell effects have been observed, providing various possible applications for our proposed system. The coherent coupling can be further extended into the USC regime with a coupling strength of 2.5 GHz measured at 37.5 GHz carrier frequency, which is a new regime where the RWA approximation may be invalidated. Compared with previous USC systems realized in microscopic and molecular structures [24–27], although our system has a relatively lower relative coupling strength (g/ω_a), it possesses narrower linewidths and thus yields an ultrahigh cooperativity of 12 000. Besides, our system has a range of other advantages thanks to the collective motion of a large number of spins and uniform magnetic coupling. The excellent tunability properties of the magnon system, together with its extended lifetime, reduced thermal excitation and the ability of coupling to microwave qubits, makes it a very promising candidate as a transducer that can interconnect different systems such as photonics, mechanics, and microwave circuits.

This work is supported by the DARPA/MTO MESO program. H. X. T. acknowledges support from a Packard Fellowship in Science and Engineering. L. J. acknowledges support from the Alfred P. Sloan Foundation, the Packard Foundation, and the DARPA Quiness program. The authors thank Dr. Michel H. Devoret and Dr. Michael Hatridge for providing a prototype 3D microwave cavity.

Note added.—While we were preparing the manuscript, another interesting work by Tabuchi *et al.* on a strongly coupled YIG-microwave cavity appeared [35].

*Corresponding author.
hong.tang@yale.edu

[1] H. J. Kimble, Nature (London) **453**, 1023 (2008).
[2] M. Wallquist, K. Hammerer, P. Rabl, M. Lukin, and P. Zoller, Phys. Scr. **T137**, 014001 (2009).
[3] R. J. C. Spreeuw, N. J. van Druten, M. W. Beijersbergen, E. R. Eliel, and J. P. Woerdman, Phys. Rev. Lett. **65**, 2642 (1990).
[4] M. Aspelmeyer, T. J. Kippenberg, and F. Marquardt, arXiv:1303.0733 [Rev. Mod. Phys. (to be published)].
[5] A. Imamoglu, Phys. Rev. Lett. **102**, 083602 (2009).
[6] J. Verdú, H. Zoubi, C. Koller, J. Majer, H. Ritsch, and J. Schmiedmayer, Phys. Rev. Lett. **103**, 043603 (2009).
[7] A. W. Eddins, C. C. Beedle, D. N. Hendrickson, and J. R. Friedman, Phys. Rev. Lett. **112**, 120501 (2014).
[8] X. Zhu *et al.*, Nature (London) **478**, 221 (2011).
[9] Y. Kubo *et al.*, Phys. Rev. Lett. **105**, 140502 (2010).
[10] R. Amsüss *et al.*, Phys. Rev. Lett. **107**, 060502 (2011).
[11] Y. Kubo *et al.*, Phys. Rev. Lett. **107**, 220501 (2011).
[12] D. Marcos, M. Wubs, J. M. Taylor, R. Aguado, M. D. Lukin, and A. S. Sørensen, Phys. Rev. Lett. **105**, 210501 (2010).
[13] V. Ranjan, G. de Lange, R. Schutjens, T. Debelhoir, J. Groen, D. Szombati, D. Thoen, T. Klapwijk, R. Hanson, and L. DiCarlo, Phys. Rev. Lett. **110**, 067004 (2013).
[14] D. I. Schuster *et al.*, Phys. Rev. Lett. **105**, 140501 (2010).
[15] S. Probst, H. Rotzinger, S. Wünsch, P. Jung, M. Jerger, M. Siegel, A. V. Ustinov, and P. A. Bushev, Phys. Rev. Lett. **110**, 157001 (2013).
[16] A. Tkalčec, S. Probst, D. Rieger, H. Rotzinger, S. Wünsch, N. Kukharchyk, A. D. Wieck, M. Siegel, A. V. Ustinov, and P. Bushev, Phys. Rev. B **90**, 075112 (2014).
[17] O. O. Soykal and M. E. Flatté, Phys. Rev. Lett. **104**, 077202 (2010).
[18] O. O. Soykal and M. E. Flatté, Phys. Rev. B **82**, 104413 (2010).
[19] S. O. Demokritov, V. E. Demidov, O. Dzyapko, G. A. Melkov, A. A. Serga, B. Hillebrands, and A. N. Slavin, Nature (London) **443**, 430 (2006).
[20] H. Huebl, C. W. Zollitsch, J. Lotze, F. Hocke, M. Greifenstein, A. Marx, R. Gross, and S. T. B. Goennenwein, Phys. Rev. Lett. **111**, 127003 (2013).
[21] H. Paik *et al.*, Phys. Rev. Lett. **107**, 240501 (2011).
[22] D. Ristè, M. Dukalski, C. A. Watson, G. de Lange, M. J. Tiggelman, Ya. M. Blanter, K. W. Lehnert, R. N. Schouten, and L. DiCarlo, Nature (London) **502**, 350 (2013).
[23] G. Kirchmair, B. Vlastakis, Z. Leghtas, S. E. Nigg, H. Paik, E. Ginossar, M. Mirrahimi, L. Frunzio, S. M. Girvin, and R. J. Schoelkopf, Nature (London) **495**, 205 (2013).
[24] B. Askenazi, A. Vasanelli, A. Delteil, Y. Todorov, L. C. Andreani, G. Beaudoin, I. Sagnes, and C. Sirtori, New J. Phys. **16**, 043029 (2014).
[25] A. Delteil, A. Vasanelli, Y. Todorov, C. Feuillet Palma, M. Renaudat St-Jean, G. Beaudoin, I. Sagnes, and C. Sirtori, Phys. Rev. Lett. **109**, 246808 (2012).
[26] G. Scalari *et al.*, Science **335**, 1323 (2012).
[27] T. Schwartz, J. A. Hutchison, C. Genet, and T. W. Ebbesen, Phys. Rev. Lett. **106**, 196405 (2011).
[28] C. Ciuti, G. Bastard, and I. Carusotto, Phys. Rev. B **72**, 115303 (2005).
[29] T. Niemczyk *et al.*, Nat. Phys. **6**, 772 (2010).
[30] G. D. Fuchs, V. V. Dobrovitski, D. M. Toyli, F. J. Heremans, and D. D. Awschalom, Science **326**, 1520 (2009).
[31] A. A. Anappara, S. De Liberato, A. Tredicucci, C. Ciuti, G. Biasiol, L. Sorba, and F. Beltram, Phys. Rev. B **79**, 201303 (2009).
[32] E. G. Spencer, R. C. LeCraw, and R. C. Linares, Phys. Rev. **123**, 1937 (1961).
[33] T. Holstein and H. Primakoff, Phys. Rev. **58**, 1098 (1940).
[34] See Supplemental Material at http://link.aps.org/supplemental/10.1103/PhysRevLett.113.156401 for the coupling strength and oscillation dynamics calculation, the comparison of the measured and calculated spectra, and a summary of the device parameters.
[35] Y. Tabuchi, S. Ishino, T. Ishikawa, R. Yamazaki, K. Usami, and Y. Nakamura, Phys. Rev. Lett. **113**, 083603 (2014).